# The Knee: Theory and Experiment.

**Gaurang B Yodh**

University of California Irvine, Irvine, CA, USA
Email: gyodh@uci.edu

**Abstract.** A review of current status of theoretical paradigm and results of direct and indirect experiments to study cosmic rays through the knee region are presented and discussed. There is general agreement that the knee is around a PeV and that it reflects a rigidity cutoff. The composition of cosmic rays in the knee region is mixed and changing with energy. The two direct experiments, JACEE and RUNJOB with measurements in the 100 TeV per particle to 1000 TeV per particle and with similar exposures do not agree. While JACEE indicates a increase in <lnA> from its low energy value of 1.5 to a value closer to 3 , the RUNJOB experiment sees no change in the composition albeit with large uncertainty. Of the indirect experiments, KASKADE, SPASEAMANDA, HEGRA- Airobic, CACTI, TUNKA and Tibet favor " Heavy " composition above the knee and beyond. The KASKADE energy range extends to 100 PeV where their analysis indicates iron dominance. KASKADE does not see a proton rigidity cutoff until about 3 PeV, while Tibet measures a steepening of the proton slope at a few hundred TeV. BLANCA and DICE favor little composition change or a change towards a proton dominated composition around 10 PeV. We need experiments with much better mass resolution in the energy range of the knee and a more quantitative understanding of the hadron production in the forward region at these energies to make definitive progress.

## 1. Introduction

The cosmic ray spectrum is relatively “smooth” from TeV to EeV, with a steepening in the PeV energy range by a relatively small increment in the slope from -2.75 to about -3.2. There are no obvious ' kinks ' or a 'bumps' in the spectrum.

Peter's pointed out [1] that if the cosmic ray spectra steepen due to a mechanism which depends on magnetic rigidity (either because the acceleration is exhausted in a rigidity dependent manner or is a result of rigidity dependent propagation) one expects systematic changes in the cosmic ray composition through this region. Current models of cosmic rays origin, acceleration and propagation postulate that there are at least two components present in galactic cosmic rays. The models may be summarized as follows:

a. One component which is due to SN explosions leading to diffusive shock wave acceleration of the ISM and another component due to

these shocks exploding into stellar winds [2].

b. A major component due to diffusive shock acceleration of the ISM and another smaller component due to a recent local SN nearby [3].

Such two component models require ' fine tuning ' in order not to produce 'kinks' or ' bumps' when one acceleration fails and the other takes over. There have been attempts to circumvent such problems by invoking only a single mechanism for explaining cosmic ray acceleration both 'below and above ' the knee [4].

In order to make progress, we need good measurements of the chemical composition of cosmic rays through the knee region. As direct measurements above the atmosphere can barely reach the knee due to paucity of cosmic ray flux and “small apertures” of these experiments we have to rely on indirect air shower based experiments to determine the nature of composition change through the knee.

The major thrust of my paper is to assess how well have indirect experiments addressed this important question. I also outline the results from direct measurements till this review.

The current paradigm for galactic cosmic ray origin can be summarized as follows: (1) Supernova explosions provide the energy source for cosmic rays, (2) shock acceleration leads to universal power law with a slope of about -2.1, (3) observed spectra are steepened from -2.1 by energy dependent path length distribution for propagation from source to earth, (4) shock acceleration terminates at energies which are ~ Z (300 TeV) determined by properties of the shocks, (5) shock acceleration and leakage out of the galaxy result in rigidity cutoff models,(6) sources have elemental abundance of the ISM or of stellar winds into which shocks travel and (7) sharpness of the cutoff depend on the details of these models. Three theoretical problems actively being pursued are: (1) Origin of knee, (2) the smoothness of transition to a steeper spectrum beyond the knee and (3) smallness of the anisotropy around the knee.

This paradigm leads to the following consequences (1) Composition of primary cosmic rays is mixed, (2) it becomes heavier as the knee is traversed, (3) the knee is around a PeV and extends over a decade in energy (4) isotropy is a consequence of pitch angle scattering in magnetic fields in the galaxy.

Consider two models in which the proton rigidity cutoff differs by a factor of 10 (0.3 PeV and 3 PeV) and ask what is the maximum difference in the average of lnA between them, one gets about 0.4. Experiments have to have a mass resolution, which can measure this difference to distinguish different composition changes predicted by different models. This task is much more difficult than asking whether composition is mostly protons or mostly iron nuclei or that it is changing.

Let us now see how well we have done experimentally. I start with results from direct experiments that should help us anchor the composition mix below the knee.

## 2. Direct Experiments

These experiments, done at balloon altitude or in space orbit, measure elemental charge Z, energy E and direction of cosmic ray particles. The fractional charge resolution is 0.2 and the energy resolution is of the order of 20% in well-designed experiments. Experiments using calorimetric techniques for energy measurements include pioneering experiments of the GSFC group [5] in balloons, Proton satellite experiment [6]. Grigorov's measurements reached the knee and a little beyond but with limited charge and energy resolution. Other calorimetric experiments include emulsion chamber instruments, such as JACEE [7], RUNJOB [8] which

accumulated enough exposure to just reach knee and ATIC [9] which had good charge and energy measurements but below the knee. Experiments have also have incorporated Transition Radiation Detectors and gaseous Chereknov counters for energy measurement such as CRN [10], on the space shuttle and TRACER [11] balloon instrument which have excellent charge resolution, and reasonable energy reach up to Lorentz factors of greater than 10,000.These instruments do not sample the elements below Boron. A compilation of recent direct measurements is shown in Figure 1.

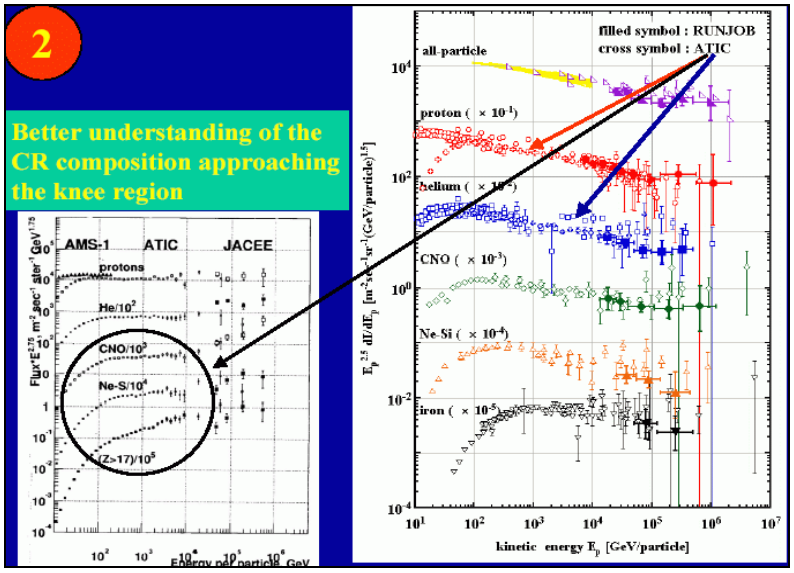


**Figure 1.** Summary of Direct measurements including JACEE, ATIC, AMS-1 and RUNJOB. The left figure ordinate is multiplied by $E^{2.75}$ while the one on the right has it multiplied by $E^{2.5}$. The right plot includes low energy AMS data. The left figure shows that according to JACEE the He and CNO group spectra seem to become harder above 100 TeV and the iron spectral index is ~-2.6 over the whole energy range.

In the above data collection, JACEE continuation beyond ATIC and RUNJOB continuation differ. This difference is displayed in Figure 2 in which average lnA versus log10 (energy). It is clear from this plot that the composition is mixed, at energies below about 100 TeV per particle <lnA> ~1.5 and constant, while above 100 TeV JACEE data indicates enhancement of heavies while RUNJOB shows no change. It clearly shows the need for experiments, which have the kind of charge resolution JACEE had and sufficient exposure to make statistically significant determinations. Also of considerable interest is to extend the measurements of secondary to primary ratio (B/C) too much higher energies. We look forward to new data from future TRACER (TRD) [11] experiment and CREAM (TRD + tracking Calorimeter) [12] experiments.

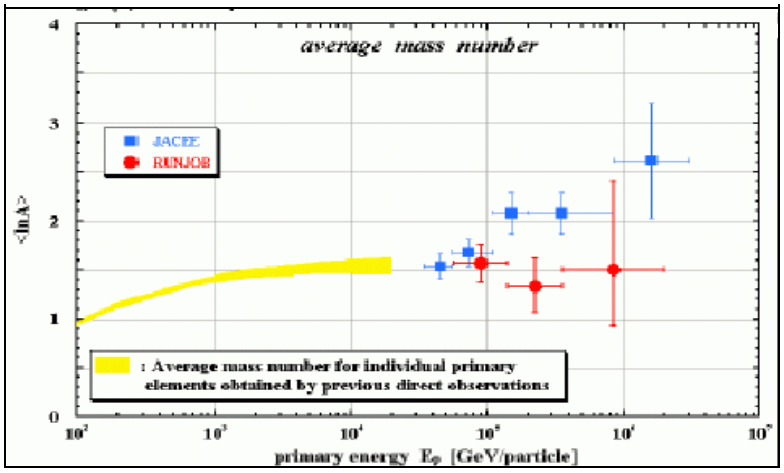


**Figure 2.** Average lnA as a function of energy for JACEE and RUNJOB experiments as compared to lower energy results.

## 3. Higher Energies: Indirect Experiments

These experiments use the atmosphere as an amplifier to enlarge the sphere of influence of cosmic rays with energies above the knee and also as a calorimeter to measure energy. The identity of the primary cosmic ray, however, has to be inferred from detailed air shower simulations. Air shower experiments are of three types:

a. Those which measure the profile of the cascade and total energy deposit by sampling either Cherenkov radiation or air fluorescence event by event (HiRes [13], DICE [14], BLANCA [15], CACTI [16], TUNKA [17]).
b. Those which measure the particles in the shower at some observation level, their lateral distribution, their energy and their time of arrival (KASKADE [18], TIBET [19], MSU [20], Akeno [21], KGF [22]).
c. Those that simultaneously measure the longitudinal and lateral profiles event by event. (BLANCA [15], HiRes-CASA [13]).

Experiments like AUGER that also fall under the third category, which are designed for higher energies are not covered in this review.

Before discussing the air shower results for spectra and composition, a discussion about sensitivity of air shower measurements to mass and energy of the primary is outlined. To describe an air shower fully requires complete knowledge of shower particles and shower photons – their energy, lateral position, longitudinal position and propagation time. Particle species include nucleons, pions, kaons, muons, electrons and positrons, gamma rays and neutrinos. Photons in the shower are due to Cherenkov radiation (beamed), air fluorescence, and radio emission due to charge separation. No experiment measures the shower fully. Shower characteristics fluctuate from event to event. Majority of the fluctuation arises from the variations in the point of first interaction. Experiments that measure the longitudinal development do not sample the point of first interaction but the position of shower maximum, called $X_{max}$. The value of depth of shower max fluctuates event by event but also is a function of total energy of the primary E and atomic mass of primary A. Usually what is studied is the average value of $< X_{max} >$ as a function of measured value of energy. The sensitivity to A and E and particle physics of Xmax can be expressed [23,24] using the superposition model as

$$< X_m(E, A) > = X_1 + (1 - B) X_0 \text{ (ln E- <lnA>)}$$

where average value of A accounts for changing composition as a function of energy. $X_1$ is model dependent but energy and A independent, however, B depends on particle physics, and $X_0 = 37\, gm/cm^2$ Elongation rate is defined as the rate of variation of depth of shower max per decade in energy. For B=0.23 and constant composition it is 66 gm/cm^2. For a composition which changes from pure O to pure P it is 84 gm/cm^2. For a given particle physics model the depth of shower max varies linearly with ln E with approximately the same slope for all pure elemental species from protons to iron. A changing composition will result in a slope different from that of the pure species: for situation when composition changes from heavier to lighter the slope is steeper and if it becomes heavier with energy the slope is flatter.

Air shower simulations using the best-known particle physics model are used to predict the expected variation of depth of shower max with energy and atomic mass. Other variables that are sensitive to atomic mass are the muon to electron content, Cherenkov lateral distribution, hadron content and its time structure. It is therefore essential to measure the atomic mass of each event by at least two independent methods – say muon/electron ratio and Xmax methods.
This will be clear as I present a compilation of recent results from different techniques.

**4. Air Cherenkov air shower experiments**

First, I present the results from experiments, which sample the longitudinal development of Cherenkov emission from the shower. Generally, these experiments determine air shower cores from ground based particle arrays and then sample the Chereknov light from the showers at different distances from the core (CACTI [16], BLANCA [15], TUNKA [17], HEGRA [25] are representative experiments), or by measuring the Cherenkov light images or fluorescence from different slant depths of the shower (DICE [14], HiRes-CASA [22] experiments).

In order to show the mass resolution from such experiments I briefly describe the CACTI experiment as illustration of the technique. In the CACTI experiment, six Cherenkov receivers were placed at suitable distances in the CYGNUS array to be able measure the Cherenkov photon density at 40 m and 140 m from the position of the shower core and size determined by the CYGNUS array. The ratio of photon densities at 40 m over that at 140 m is sensitive to atomic mass of the primary. The observed distribution of this ratio is sensitive to A and the sensitivity is shown in Fig. 3 where data is compared to simulations for different A.

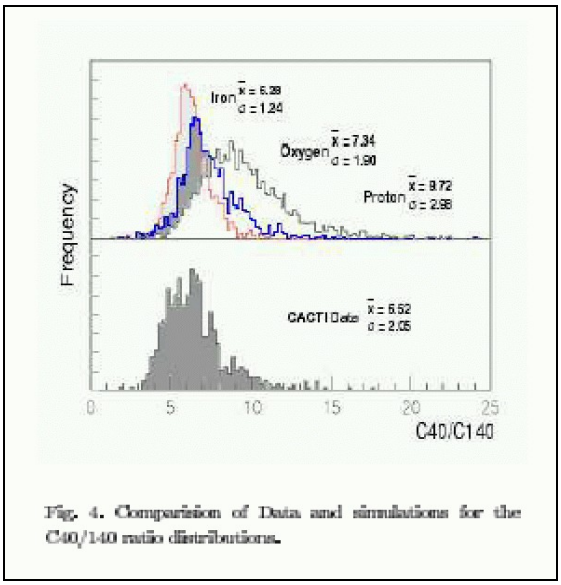


Fig. 4. Comparision of Data and simulations for the C40/140 ratio distributions.

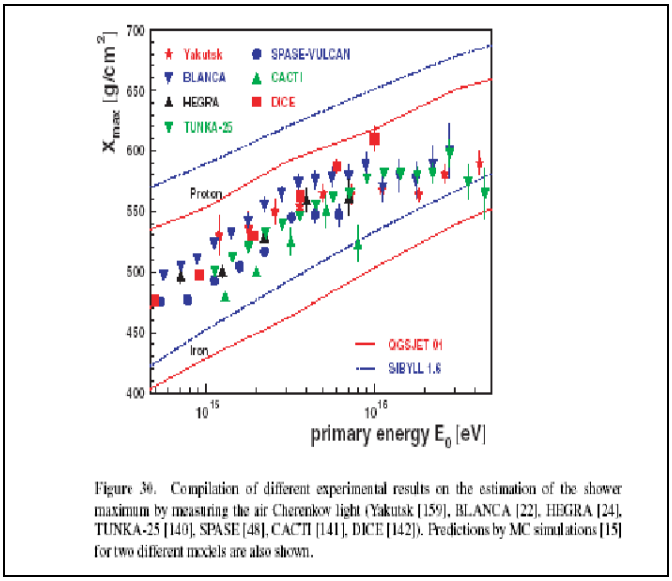


Figure 30. Compilation of different experimental results on the estimation of the shower maximum by measuring the air Cherenkov light (Yakutsk [159], BLANCA [22], HEGRA [24], TUNKA-25 [140], SPASE [48], CACTI [141], DICE [142]). Predictions by MC simulations [15] for two different models are also shown.

**Figure 3.** Comparison of data and simulations for the photon density ratio, C(40m)/C(140m), distributions for fixed zenith angle showers.
**Figure 4.** Xmax measurements as a function of energy in knee region from various experiments.

The average value of this ratio for showers coming from a fixed zenith angle can be related to the depth of shower maximum also. The energy of the shower is determined from the shower size obtained by the CYGNUS experiment. The mass resolution is not sufficient to separate the species but can be used to estimate the average lnA in the energy range of the experiment (Paling, et al.).

Most of the air shower experiments in this energy range which measure properties of the Cherenkov radiation to extract Xmax and average lnA (DICE, BLANCA, HEGRA, TUNKA, SPASE-AMANDA [26]) have similar mass resolutions. Their results are summarized in Fig. 4, which plots Xmax vs. energy. For comparison the simulated variation of Xmax with energy for proton and iron primaries, for two different hadronic models, is also shown.

I draw four conclusions from Figure 4: (1) All results are consistent with a mixed composition near 1 PeV and (2) Composition is changing between 1 and 10 PeV and (3) systematic differences between experiments are much larger than the errors quoted and (4) there is no consensus on the direction of change of the composition, that is on the elongation rate of Xmax, in this energy range. There is general agreement between HEGRA-AIROBIC, CACTI and TUNKA, while these experiments differ from BLANCA and DICE. The second set of experiments indicate a lighter composition at 10 PeV while the first set favor a heavier composition at 10 PeV.

Air shower experiments which measure the properties of shower particles in an air shower particle array also can extract average lnA from their measurements and these are discussed next.

## 5. Ground Based Air Shower Experiments

There have been ground based extensive air shower experiments since the end of the World War II, which have explored cosmic rays with energies above 100 TeV. They are too numerous to cover in this short review, so I will concentrate on a few of them. In earliest of these the array sampled electromagnetic and muonic

components to extract the shower energy and primary composition of the showers. Usually, as electrons and gamma rays are more numerous than muons the shower trigger used was based on electrons detected or Ne. The ratio of number of muons in a shower Nmu to Ne is used to estimate average primary mass for fixed Ne at some fixed zenith angle (for example Tien Shan [27] and KGF [22]). Triggering on total Ne enhances proton fraction in triggered events because of deeper penetration of protons before shower develops (larger Xmax) and makes the method less sensitive to heavier nuclei. Other experiments study equal intensity curves to find average depth of maximum (Chacaltaya [28]). This method has difficulties if the composition is changing because equal intensity does not correspond to equal energy on an event-by-event basis. Another method was to study the fraction of delayed energetic hadrons (nucleons) near air shower cores (Goodman et al [29]). The results from these experiments near the knee ranged from ' constant composition models' which did not favor a rigidity dependent cutoff (Tien Shan [27]), to ' iron enhanced models "  which favored a rigidity cutoff origin of the knee with the proton rigidity cutoff at about 0.3 to 0.5 PeV (Goodman et al[29]).

The knee region has been covered by a number of air shower arrays in the last several decades. They all sample two or more components of the shower particles at observation level and determine Ne and Nmu and Nh (high energy hadrons calorimetrically). A partial list is: AKENO (Ne,Nmu) [21], CASA-MIA (Ne,Nmu) [30], EAS-TOP (Ne, high energy Nmu [31]), KGF (Ne, high energy Nmu [22]), SPASE-AMAMDA (Ne, Nmu) [26], HEGRA (Ne,Nmu,C) [25], KASKADE (Ne,Nmu,Nh) [18] and TIBET (Ne,Nh) [19],GRAPES (Ne,Nmu) [32]. I will discuss the two experiments currently operating in the knee region – from 0.1 PeV to 100 PeV. I will briefly present their analysis techniques and their results before discussing the totality of all results relating to the determination of energy variation of <lnA> as a function of E.

*5.1. KASKADE Experiment*

This is a well-instrumented and appropriately spaced air shower array to study the composition and energy spectra of cosmic rays in the knee region. It measures the lateral distributions of electrons and muons with scintillation counters and also samples the hadronic component of the shower and some high-energy muons in a centrally located segmented calorimeter. The KASKADE experiment is shown in Fig. 5.

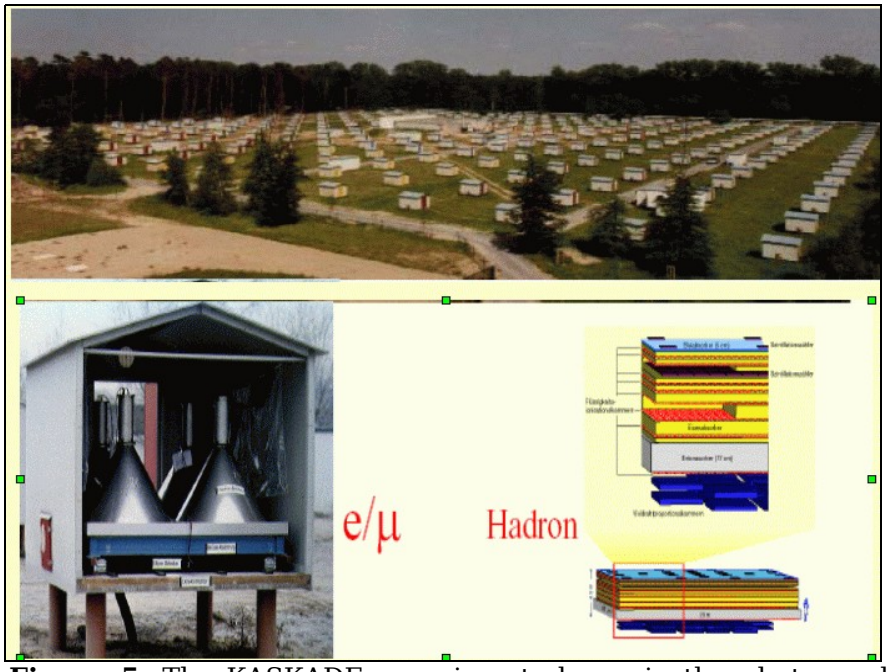


**Figure 5.** The KASKADE experiment shown in the photograph on the top. The bottom pictures show the details of the stations measuring the electron and muon components and of the central calorimeter. The figure on left is for e and mu and the one on right is the calorimeter.

They use a combination of measured values of $N_e$ *and* $N_\mu^{trunc}$ to estimate energy of the shower based upon their simulations in the energy range of the knee. The mass composition and elemental energy spectra are determined from the scatter plot of $\log N_\mu^{trunc}$ *versus* $\log N_e$ . Truncated refers to the muon number within the array. The distribution is analyzed as an inverse problem to find energy spectra of different elements. The truncated muon number is a robust parameter with respect to fluctuations of the depth of shower maximum. They also use hadron-electron and hadron-muon correlations to determine the composition. Their analysis is summarized in Figure 5. These and other analysis techniques are described in review by Haungs, Rebel and Roth [33].

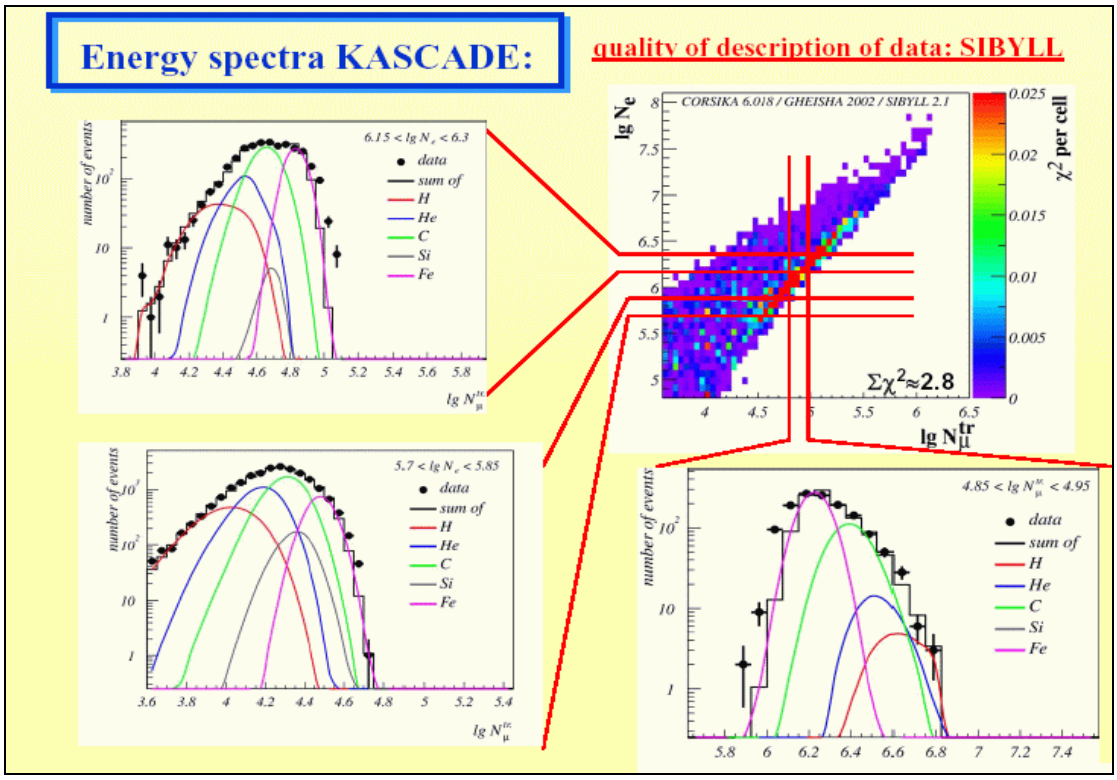


**Figure 6.** Illustration of the KASKADE technique for extracting elemental spectra.

The derived elemental spectra depend on the assumed hadronic models in their simulations. The spectra calculated for the QGS-jet model and for SIBYLL-2.1 model are shown in Fig. 6. Both analyses give an all particle spectrum that agrees reasonably well with measurements; however, the spectra of individual components are quite different in the two cases. It shows the difficulty in extracting information about primary cosmic rays from ground level air shower experiments.

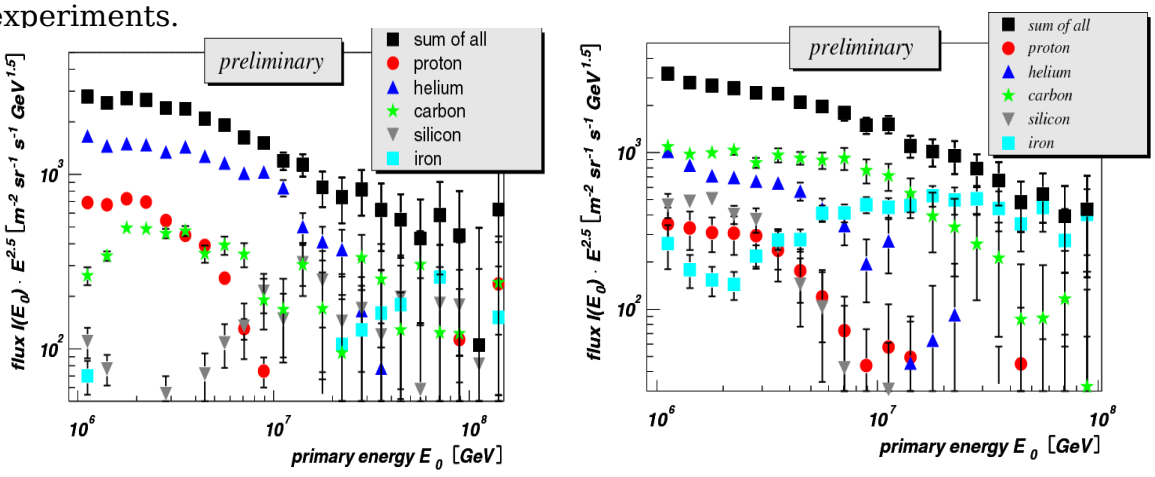


QGS-jet SIBYLL-2.1

**Figure 7**. Elemental spectra derived from analysis of Ne vs. Nmu scatter plot of KASKADE experiment for two different hadronic interaction models. Note the considerable differences for the resulting elemental spectra.

KASKADE experiment obtains a rigidity dependent cutoff, which for protons is about 3 PeV. This is an order of magnitude higher than that obtained by the delayed hadron experiment mentioned earlier. Knowing the elemental spectra one can calculate the energy variation of <lnA> with energy. These results are discussed a little later.

*5.2. The Tibet Experiment*

The Tibet experiment, which is located at 4300 m can estimate shower energies through their shower size measurements with less sensitivity to fluctuations of shower max, as their altitude is near to Xmax in the knee region. The Tibet array is shown in Fig. 7. The experiment measures the electron lateral distribution and determines the shower size for each event whose core lies within the array. They also measure the high-energy hadronic component by means of an array of burst detectors which sample the hadronic cascade by high-energy hadrons in the shower using a scintillation counter below a layer of lead and also emulsion chambers, which can measure the burst through cascade development. Fig. 9 shows a photograph of the burst arrangement and a schematic of the X-ray film emulsion detector above the burst detectors.

The Tibet collaboration did detailed simulations to study the effectiveness of burst detectors in discriminating proton initiated showers from those initiated by other nuclei and developed a method to find proton induced showers and then measure their spectrum. Their result shows a proton spectrum whose slope steepens above an energy of about 0.3 PeV. This is shown in Fig. 10.

**Figure 8.** A photograph of the Tibet array at an altitude of 4300 m. The white objects is scintillation counter array with the central station containing the hadron detetectors, which are burst and emulsion chamber units.

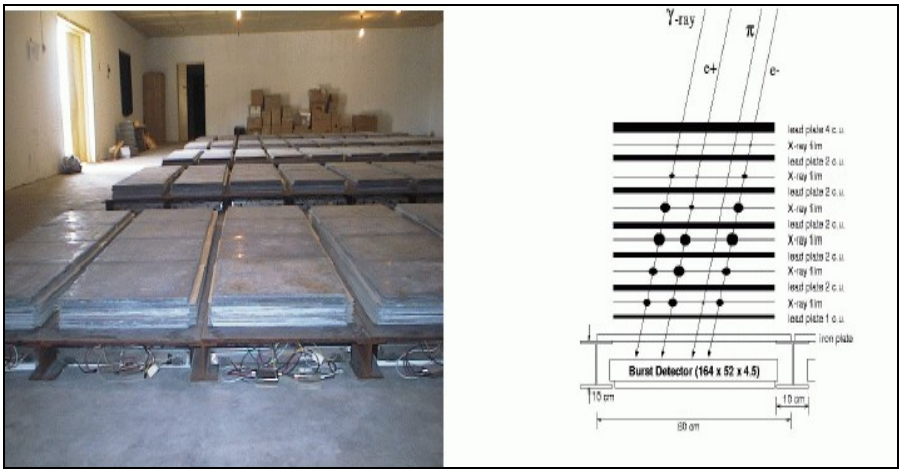


**Figure 9.** Central burst detector showing the X-ray film emulsion blocks burst counters. **Figure 10.** The tibet proton spectrum derived using different analysis methods. The Tibet all particle spectrum compared to AKENO spectrum in the knee region is also shown. The proton spectrum

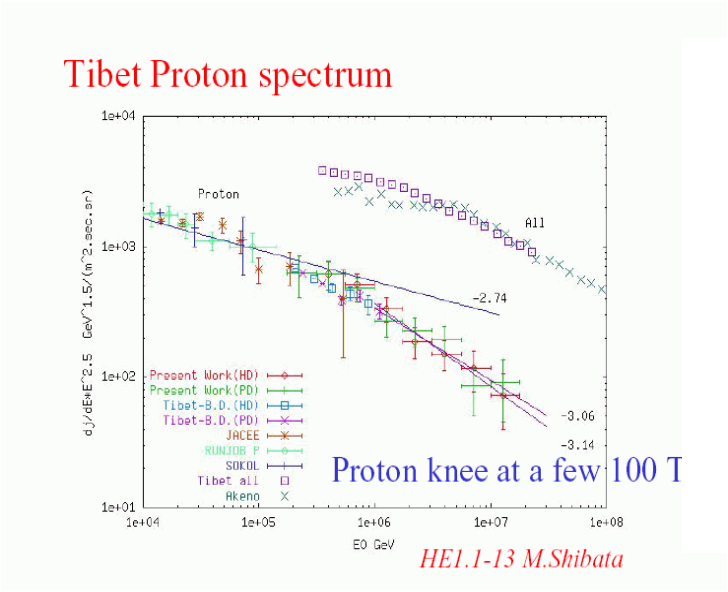


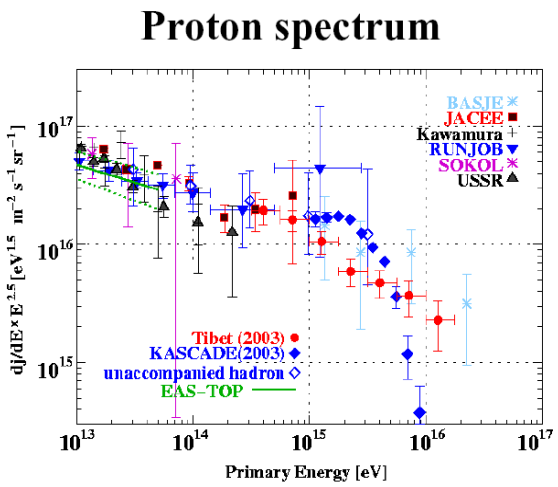


steepens at few 100 TeV.

**Figure 11.** Air Shower measurements of the proton spectra compared with direct measurements.

A compilation of direct measurements of the proton spectra and their continuation according to Tibet and KASKADE experiments is shown in Fig. 11. Just as in Figure 10, the differential spectrum is multiplied by $E^{2.5}$ in this figure. Possible systematic differences in energy determination by different experiments is not included in this plot. For the indirect experiments the derived result depends on the simulation models which are not the same for the Tibet and KASKADE analyses. The KASKADE result shows a much sharper cutoff at a higher energy than the Tibet experiment which shows a spectral steepening of about -0.5 at a

lower energy. Finally, I present the current status of determination of energy variation of <ln A> from the indirect experiments done by various experiments. In Figure 12, a partial summary of the results is shown.

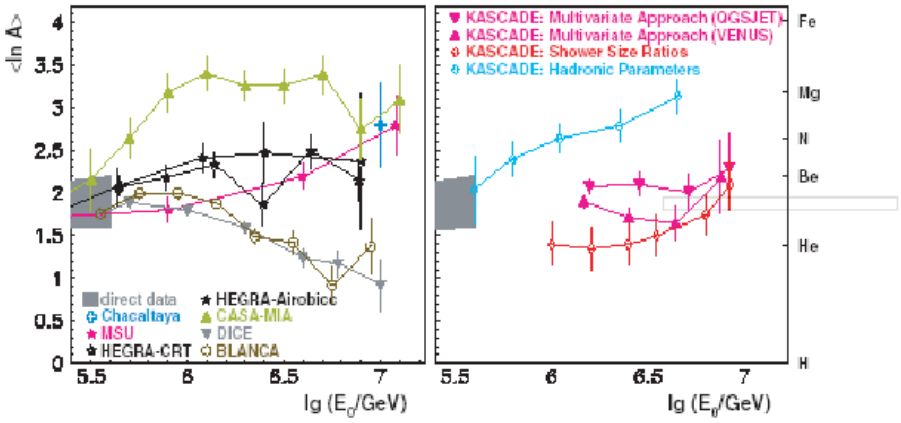


**Figure 12.** A comparison of energy variation of <lnA> with energy from the KASKADE experiment using different techniques compared with earlier determinations (Haungs, Rebel and Roth [33]).

An examination of Figure 12 leads one to the conclusion that indeed the extraction of cosmic ray composition from indirect experiments between 0.3 PeV and 10 PeV is very difficult. The indirect results are anchored to direct measurements but start to diverge at higher energies. At 10 PeV, DICE and BLANCA are consistent with a helium dominated composition while others range from Be to Mg dominated composition. Unfolding procedure of the KASKADE data alone, combined with neural network analysis gives results which imply "iron" dominance by 100 PeV (Haungs, Rebel and Roth [33]). A final summary of most of the measurements, direct and indirect is shown in Figure 13 taken from TAKITA's summary at Tsukuba(Takita 2003[34]).

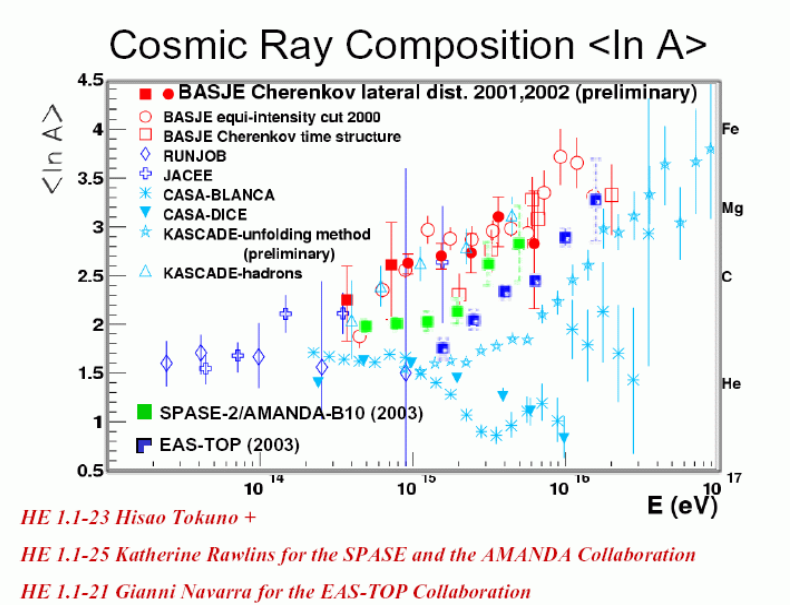


*HE 1.1-23 Hisao Tokuno +*

*HE 1.1-25 Katherine Rawlins for the SPASE and the AMANDA Collaboration*

*HE 1.1-21 Gianni Navarra for the EAS-TOP Collaboration*

**Figure 13.** A compilation of <lnA> versus energy from direct and indirect experiments covering energy range $10^{13} eV \ \ to 10^{17} eV$.

Examination of this figure shows that the inverse problem of deriving the mass composition of cosmic rays from indirect experiments is, to say the least, quite difficult and one cannot derive any definite conclusions about the change or the rate of change of composition in the energy range from 0.1 PeV to 100 PeV.

## 6. Conclusions

There is general agreement that the knee in the all particle spectrum is between 1 and 5 PeV. It represents a steepening of the all particle spectrum from -2.75 to -3.2 over an decade in energy. The two direct experiments, JACEE and RUNJOB with measurements in the 100 TeV per particle to 1000 TeV per particle and with similar exposures do not agree. While JACEE indicates a increase in <lnA> from its low energy value of 1.5 to a value closer to 3 , the RUNJOB experiment sees no change in the composition albeit with large uncertainty.

Of the indirect experiments, KASKADE, SPASE-AMANDA, HEGRA-Airobic, CACTI, TUNKA and Tibet favor " Heavy " composition above the knee and beyond. The KASKADE energy range extends to 100 PeV where their analysis indicates iron dominance. KASKADE does not see a proton rigidity cutoff until about 3 PeV, while Tibet measures a steepening of the proton slope at a few hundred TeV. BLANCA and DICE favor little composition change or a change towards a proton dominated composition around 10 PeV.

In my opinion, the knee is there but its details are still elusive. Rigidity cutoff is a likely scenario, but not resolved experimentally. One needs experiments which can determine the longitudinal development and lateral distributions event-by-event with sufficient redundancy and precision to be able to achieve a mass resolution much better than currently obtained. One needs a resolution $\frac{\Delta A}{A} << 1$ to separate the elements. Can it be done?

If primary charge, before the nucleus generates the air shower can be determined, it would be an important step in ground-based experiments (Kieda, Swordy and Wakely [35]).

Further progress in understanding the knee needs a modern version of the Proton experiment (for instance ACCESS) orbiting the earth to cover the knee region. Improving simulations needs accelerator experiments, which quantify the forward region of hadronic interactions in order to make robust simulations.

**Acknowledgments**

This work was supported in part by the National Science Foundation. I want to thank the organizers for giving me the opportunity to relook at the ' Knee ' and the rigidity cutoff model, which I first studied in 1958.

**References**

[1] Peters B 1961 *Nuovo Cimento*, **22** 800.
[2] Biermann P 1993 *Astron.* And *Astroph*, **271** 649 and 2001 *ibid* **369** 269
[3] Wolfendale A W and Erlykin A D 1997 *Astroparticle Physics* **7** 203
[4] Axford W I 1990 *ICCR International Symposium on the Astrophysical Aspects of the Most Energetic Cosmic Rays*, Kofu, Japan, Nov. 26-29 In *Kofu 1990, Proceedings, *Astrophysical aspects of the most energetic cosmic rays** 406-420.

[5] Ryan M J ,*et al* 1972 *Phys.Rev. Letters* **28** 985
[6] Grigorov N L *et al* 1971 *12th ICRC* 5 pages: 1746, 1752,1760
[7] Burnett T H *et al* 1983 *Phys. Rev. Letters* **50** 2062*ibid* **51** 1010; *Nucl.Inst.and Methods* 1986, **A251** 583
[8] RUNJOB Collaboration, *Adv. Space Res.*2000; **26** 1839; Ichimura M *et al*, *Phys. Rev.D* 1993, **48** 1949; *Astroparticle Physics* 1997, 6 155
[9] Guzik T, *et al* (for the ATIC Collaboration) ,2004 *Adv. Sp. Res.* **33(10)** 1763 also *28th ICRC(Tsukuba)* 2003, 1833,1853,2109
[10] Muller D, *et al* 1991 *Ap.J.* 374 356
[11] Muller D, et al ; *TRACER experiment* (to be published 2005)
[12] Seo E *et al*, (for the CREAM Collaboration) , *28th ICRC (Tsukuba)* 2003, 2101.
[13] T. Abu Zayyad *et al* 2001*Astrophys.J.* **557**:686-699
[14] Swordy S P, and Kieda D B (for the DICE Collaboration) 2000 *Astroparticle Phys.* **13** 127
Boothby K, *et al* 1997, *Ap.J.Letters* **491** L35-L38
[15] Fowler J W *et al* 2001 *Astropart.Phys.* **15**:49-64
[16] Paling S and Hillas A M 1995 *24th ICRC(Rome)* **3** 508
Yodh GB (for the CACTI Collaboration) 2003 *Nucl. Phys. B(Proc. Suppl)* **122** 239
[17] Chernov D *et al* (for the TUNKA Collaboration) 2004 *Int . Journal of Modern Physics* **A**
[18] Antoni T *et al* (for the KASKADE Collaboration)2003 *Nucl. Inst.and Methods* **A513** 490
[19] Amenomori M *et al* (for the Tibet Collaboration) 2003 *28th ICRC(Tsukuba)* **1** 107
[20] Fomin Y A *et al* (for MSU) 1991 *22nd ICRC (Dublin)* **2** 85
[21] Nagano M *et al* (for the Akeno Collaboration) 1984 *J.Phys.G:Nucl.Part.Phys* **10** 1295
[22] Acharya BS *et al* (for the KGF Collaboration) 1981 *17th ICRC(Paris)* **11** 385
[23] Linsley J and Watson AA 1981, *Phys. Rev.Letters* **46** 459
[24] Walker R and Watson AA 1981, *J.Phys.G:Nucle.Phys.* **7** 1297
[25] Arqueros F *et al* (for the HEGRA Collaboration) 2000 *Astron. Astrophys* **359** 682
[26] Rawlins K *et al* (for the SPACE/AMADA Collaboration) 2004 *Astropart.Phys.* **21** 565-581
[27] Nikolski SI *et al* (for the Tien Shan Collaboration) 1979 *16th ICRC(Kyoto)* **8** 335
[28[ Ogio S *et al* (for the Chacaltaya Collaboration) 2003 *28th ICRC(Tsukuba)* **1** 131
[29] Goodman JA *et al* 1979 *Phys.Rev.Letters* **42** 854
Goodman JA *et al* 1982 *Phys. Rev.* D **26** 1043 (Delayed hadrons)
[30] Glassmacher MAK (for the CASA-MIA Collaboration) 1999 *Astropart. Phys.* **10** 291
[31] Aglietta M *et al* (for the EAS-TOP Collaboration) 1999 *Astropart. Phys.* **10** 1
[32] Tonwar SC *et al* 2003 *28th ICRC(Tsukuba)* **HE 1** 167
[33] Hanugs A Rebel H and Roth M (2003) *Rep. Prog. Phys.* **66** 1145
[34] Takita M 2003 *28th ICRC (Tsukuba)* Rapportuer talk, p 277.
[35] Kieda D, Swordy S and Wakely S 2001 *Astropart.Phys.***15** 287-303